Porous Azatruxene Covalent Organic Frameworks for Anion Insertion in Battery Cells

Sebastian M. Pallasch,[¶] Manik Bhosale,[¶] Glen J. Smales, Caroline Schmidt, Sibylle Riedel, Zhirong Zhao-Karger, Birgit Esser,* and Oliver Dumele*

ABSTRACT: Covalent organic frameworks (COFs) containing well-defined r edox-active g roups h ave b ecome competitive materials for next-generation batteries. Although high potentials and rate performance can be expected, only a few examples of p-type COFs have been reported for charge storage to date with even fewer examples on the use of COFs in multivalent ion batteries. Herein, we report the synthesis of a p-type highly porous and crystalline azatruxene-based COF and its application as a positive electrode material in Li- and Mg-based batteries. When this material is used in Li-based half cells as a COF/carbon nanotube (CNT) electrode, a discharge potential of 3.9 V is obtained with discharge capacities of up to 70 mAh g^{-1} at a 2 C rate. In Mg batteries using a tetrakis(hexafluoroisopropyloxy)borate electrolyte, cycling proceeds with an average discharge voltage of 2.9 V. Even at a fast current rate of 5 C, the capacity retention amounts to 84% over 1000 cycles.

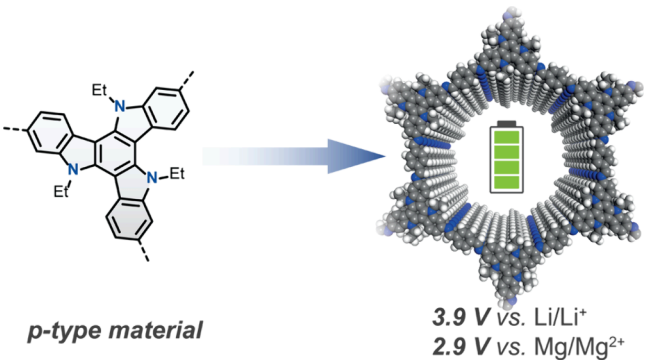

INTRODUCTION

Because of climate change, there is an urgent need to develop reliable energy storage devices that use abundant or even sustainable materials and that are safe and have long lifetimes. Such devices will have great utility for storing electrical energy produced from renewable and clean resources, such as biomass, solar, wind, and hydropower plants, that are sometimes restricted with time-dependent availability.[1] Hence, novel technologies and charge storage chemistries have to be developed to fulfill the criteria of a higher sustainability and safety, in particular.[2−5] Organic electrode materials are promising candidates to be used in such alternative technologies because the structural diversity in organic chemistry allows for the design of materials with tailored properties and, for example, the use of small molecules or redox polymers[6] as electrode-active materials.[7,8]

In recent years, covalent organic frameworks (COFs)[9] have become contenders as organic active materials for batteries because of their highly ordered nanoporous structure, large surface area, and diverse functionalization opportunities.[10,11] For example, COFs can be tailored to incorporate redox-active groups that, in turn, affect their charge storage properties[12] while it has also been shown that their porous structures can enhance ion diffusion.[13] Most reports on COFs as battery electrode materials use an n-type redox activity of the COF in Li-based batteries[3,14,15] with few examples of multivalent ion batteries.[16−18] However, the rate performance of n-type COFs, as well as the obtainable cell voltages, are often limited to values of up to 3 V vs Li/Li^+.[11] With p-type organic electrode materials, however, cell voltages above 4 V vs Li/Li^+ can be obtained.[11] Furthermore, the rate capability of p-type materials is often higher as anion insertion concurrent with an oxidation of the organic redox-active groups during charge is fast. Hence, the development of p-type redox-active COFs with a high operating potential is an attractive yet underexplored goal. Reported examples use (2,2,6,6-tetramethylpiperidin-1-yl)oxyl (TEMPO) as side groups to COF linkers,[19] phenoxazine COF linkers,[20] or triarylamine COF nodes[21] to show redox activities below or around 4 V vs Li/Li^+.

As an alternative to Li-based batteries, cells using multivalent metals, such as Al and Mg, are considered viable solutions because these metals are intrinsically safe for the use as negative electrode materials and are abundant in the Earth's crust.[22,23] However, the development of positive electrode materials for Al and Mg batteries is still in its infancy and faces severe challenges.[23,24] Organic electrode materials are promising candidates with high achievable high cell voltages[25] and the

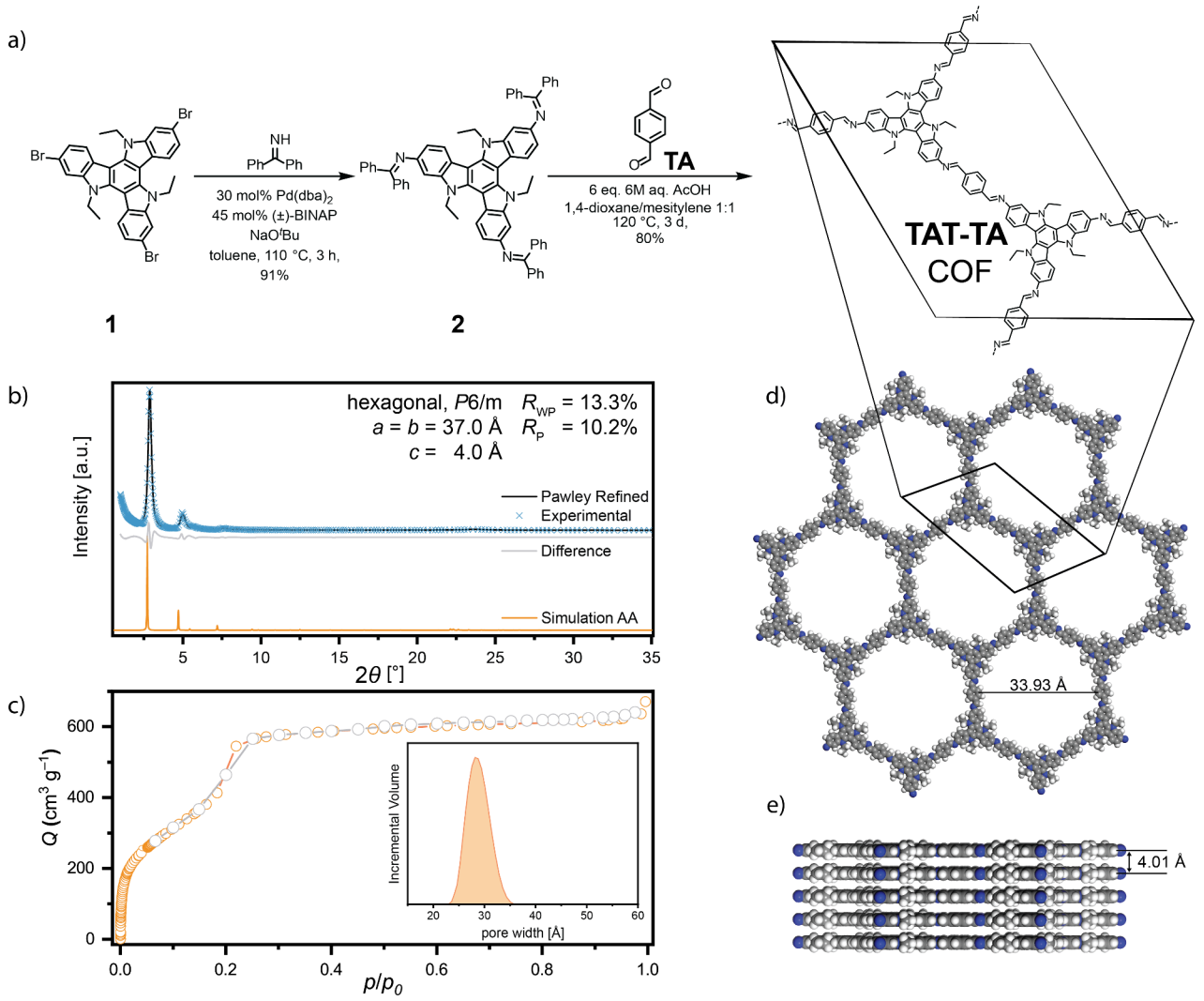

Figure 1. (a) Synthesis of azatruxene **2** and **TAT-TA** COF. (b) PXRD data of **TAT-TA** COF: experimental PXRD pattern (blue crosses), Pawley refinement (black line) using an optimized structural model (see d,e), difference between Pawley refinement and experimental data (gray line), and simulated PXRD pattern (orange). (c) N_2 sorption isotherms of **TAT-TA** COF. (d,e) Modeled three-dimensional structure of **TAT-TA** COF.

opportunity to use an anion storage mechanism with p-type redox-active groups. Recently, advanced electrolytes for Mg-based batteries have been developed that consist of non-coordinating (and non-nucleophilic) anions to the Mg salts, which can also be used with such p-type organic electrode materials. One example is the magnesium tetrakis-(hexafluoroisopropyloxy)borate ($Mg[B(hfip)_4]_2$) salt, which additionally has a high oxidative stability > 4.3 V.[26] To date, there are only three reports on p-type organic electrodes in such a dual-ion Mg cell configuration,[27−29] but there is no report yet on a p-type COF used as such. Only a triazine-based amorphous porous organic polymer (POP) and Dichtel's antraquinone COF[30] have been reported for use as n-type electrode material in Mg batteries for cation storage.[18,31] Herein, we report the first example of a p-type COF used in a Mg battery, thereby exceeding the voltage limit of 2 V in such battery cells.[32] The COF operates in an anion storage mechanism and is one of the first high-voltage p-type COFs used as electrode materials, in general. Azatruxene is employed as a heterocyclic electron-rich and redox-active scaffold with an efficient $\pi-\pi$ stacking ability, a good prerequisite for COF formation.[33−35] Triazatruxene (TAT) has previously been implemented into porous materials,[36−38] for example, in a conjugated microporous polymer for application as a fluorescence probe[36] and in a supercapacitor with a capacitance of up to 183 F g^{-1} and high cycling stability during 10 000 cycles.[38] These values are remarkable despite the low porosity and the absence of crystallinity in the reported materials. No application as battery electrode materials has yet been reported for azatruxene COFs.

RESULTS AND DISCUSSION

To obtain a crystalline COF, the transamination approach was chosen herein.[39] Tribromo-azatruxene **1**[33] was reacted with benzophenone imine in a Buchwald−Hartwig coupling to obtain 2,7,12-tris(*N*-benzophenone imine)-5,10,15-triethylazatruxene **2** as COF precursor. Trisimine azatruxene **2** was reacted with terephthalaldehyde (**TA**) under solvothermal conditions to form the 2D **TAT-TA** COF with a hexagonal lattice (Figure 1). Powder X-ray diffraction (PXRD, Figure 1b) showed several intense reflexes, which correspond to Bragg reflexes of the COF lattice and indicate high crystallinity. A simulated periodic force field model, as implemented in Materials Studio,[40] was used for the Pawley refinement of the

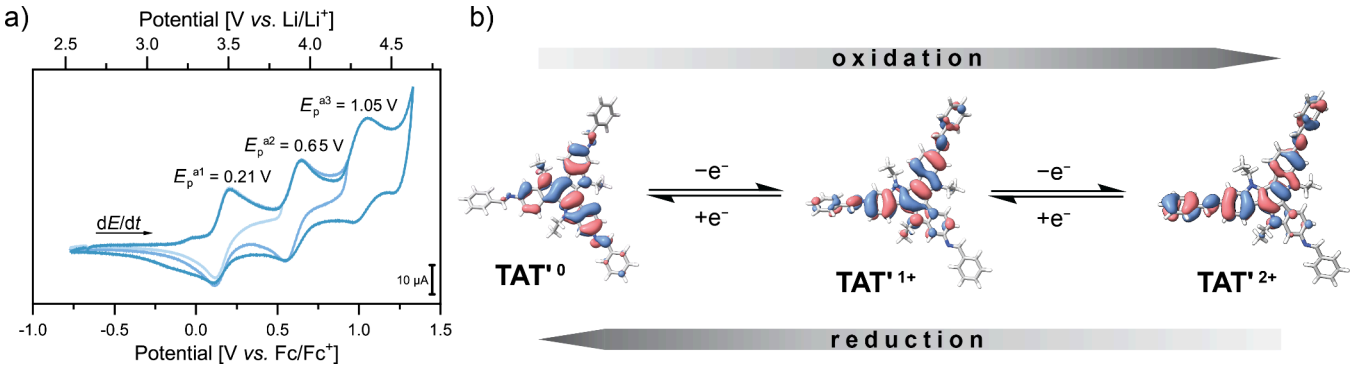

Figure 2. (a) Cyclic voltammograms of azatruxene **2** (1 mM in CH_2Cl_2 with 0.1 M n-Bu_4NPF_6, scan rate 100 mV s^{-1}, vs Fc/Fc^+), and (b) **TAT'** charged states shown as HOMO/SOMO plots.

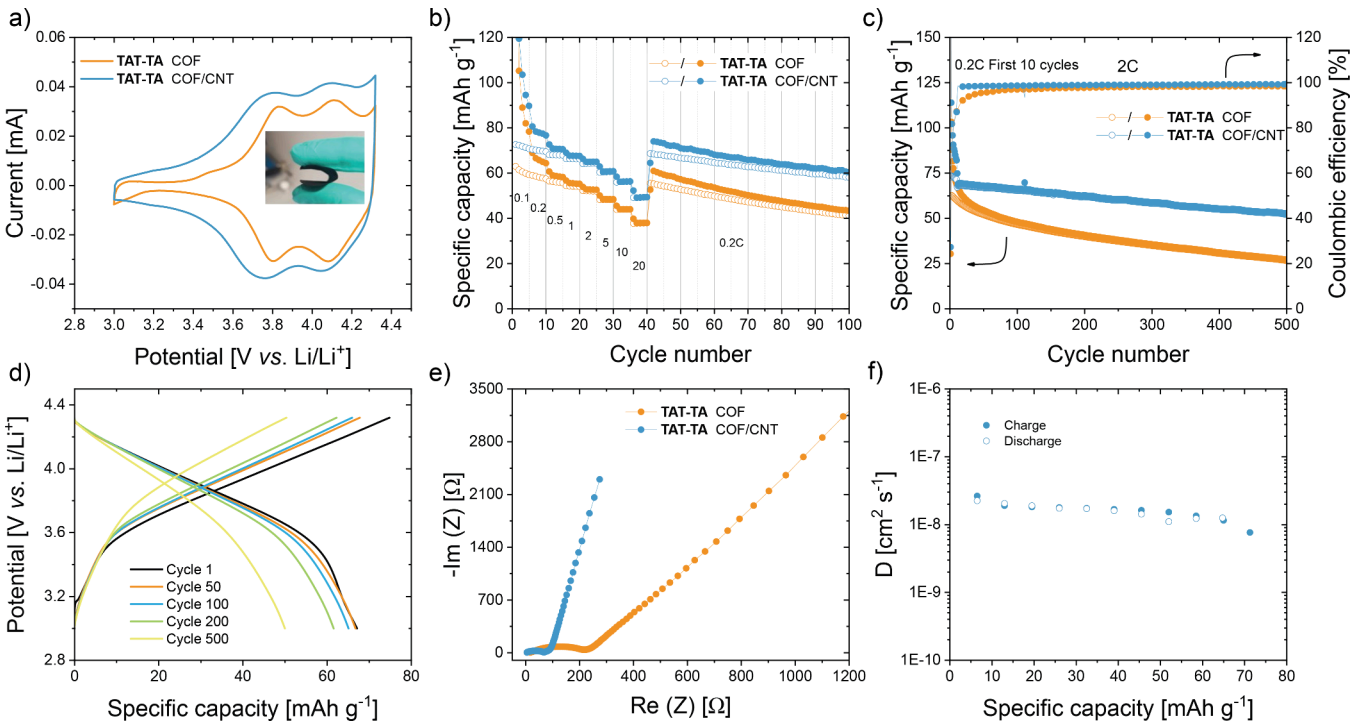

Figure 3. Electrochemical performance of **TAT-TA** COF (30/50/20 wt % COF/acetylene black/PVdF) and **TAT-TA** COF/CNT electrodes (1:2 wt ratio of COF/SWCNTs) in Li-based half cells (1 M $LiPF_6$ in EC/DMC 1:1). (a) CVs at 0.2 mV s^{-1} (cycle 10). (b) Rate capability. (c) Cycling stability at 2 C rate. (d) Selected charge/discharge curves of **TAT-TA** COF/CNT electrodes at 2 C rate. (e) Nyquist plots of **TAT-TA** COF and **TAT-TA** COF/CNT electrodes from EIS measurements. (f) Diffusion coefficients obtained from GITT measurements for **TAT-TA** COF/CNT electrodes.

experimental PXRD (Figure 1b,d,e). It shows good agreement with a hexagonal $P6/m$ space group representing an eclipsed AA stacking pattern (refined lattice parameters $a = b = 37.5$ Å and $c = 4.0$ Å). The sterically demanding ethyl groups lead to an interlayer distance of 4 Å (Figures 1e and S1e) and an average inner pore diameter of 33.93 Å (Figures 1d and S 1f). The insignificant deviation of the simulated and experimental reflex angles 2θ can be explained by the slightly nonplanar geometry of the azatruxene core confirmed by DFT calculations, which cannot be modeled with the force field of Materials Studio accurately (Supporting Information, Section S17). The reflex at $2\theta = 2.88°$ is assigned to the (100) lattice plane of the unit cell. Additional reflexes at 5.00° and 5.77° represent the (110) and (200) planes, respectively. A broad reflex is centered at around 25°, corresponding to the (001) plane and confirming the π–π stacked two-dimensional structure at an interlayer distance of around 4 Å (Figure 1b). Nitrogen adsorption isotherms indicate a mesoporous material by a type IV isotherm (Figure 1c). The experimental surface area was evaluated to 1546 m^2 g^{-1} employing the BETSI algorithm (Figure S3; $S_{BET,calc}$ = 2144 m^2 g^{-1}),[41] and the pore size distribution shows a major peak at 29 Å in good agreement with the experimentally obtained (100) reflex by PXRD (31 Å).

Cross-polarization magic-angle spinning nuclear magnetic resonance (CP-MAS NMR) and Fourier-transform infrared spectroscopy (FT-IR) were used to examine the chemical composition of **TAT-TA** COF (Supporting Information, Figures S4 and S5). The C═N imine stretch (1715 cm^{-1}) and the absence of the C═O stretch (1690 cm^{-1}) of **TA** confirmed the complete framework formation. Another indication is the absence of an aldehyde signal at around

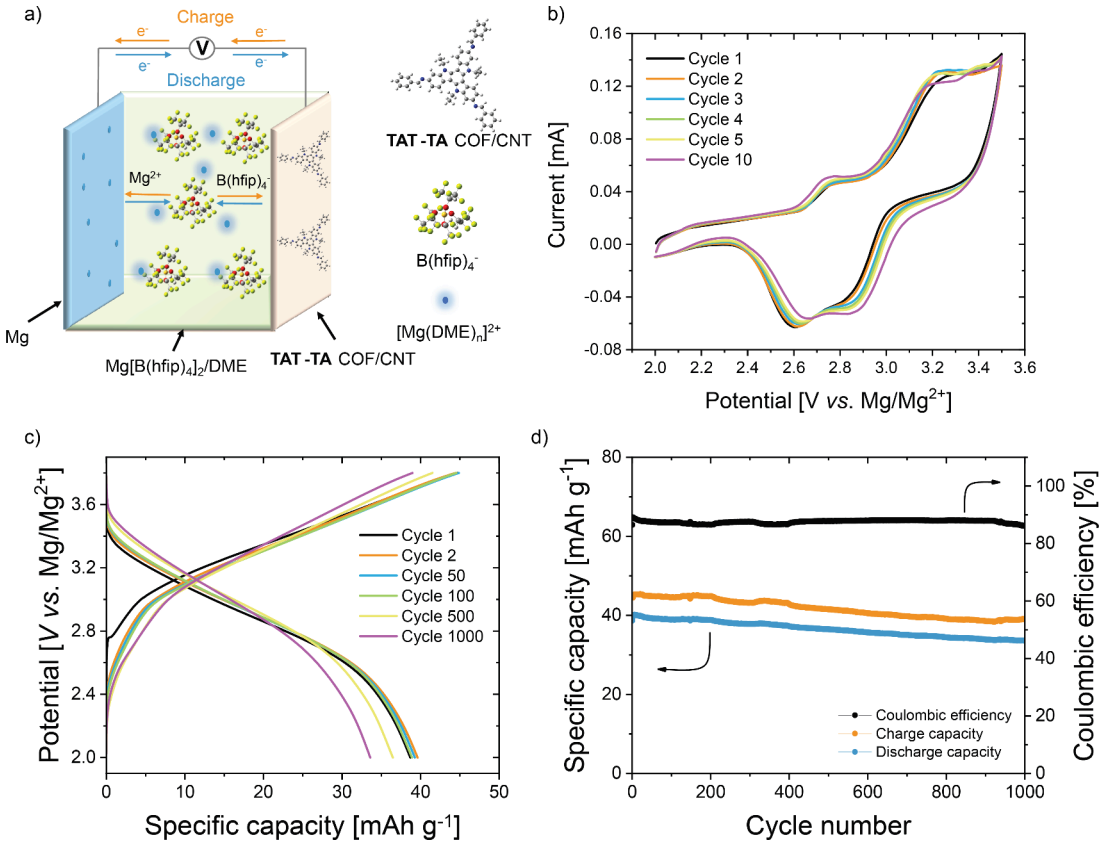

Figure 4. Electrochemical performance of **TAT-TA** COF/CNT electrodes (1:2 wt ratio of COF/CNTs) in Mg-based coin cells (0.3 M $Mg[B(hfip)_4]_2$·3DME in DME). (a) Schematic of the cell setup. (b) Cyclic voltammograms at 1 mV s^{-1}. (c) Selected charge/discharge curves during galvanostatic cycling at 5 C. (d) Cycling stability at 5 C.

200 ppm in the CP-MAS NMR spectrum. Examination of the morphology using scanning electron microscopy (SEM) revealed highly uniform aggregates of spherical particles of ~2−3 μm diameter (Figures S11 and S12).

The azatruxene tris(imine) core can undergo up to three reversible one-electron oxidations, thereby making it attractive for charge storage in batteries. In derivative **2**, these are centered at half-wave potentials of 0.21, 0.65, and 1.05 V vs Fc/Fc^+ (Figure 2a; for differential pulse voltammograms see Figure S7), and in tribromo azatruxene **1**, they are shifted to higher potentials (Figure S8). In the oxidized form, the charges are delocalized over the azatruxene core (Figure 2b), as indicated by the calculated HOMO/SOMO (singly occupied molecular orbital) of the neutral, cationic, and dicationic 2,7,12-tris(benzylimine)-*N*,*N*′,*N*″-triethylazatruxene model **TAT'** (Figure 2b) and in its various charged states (Section S17). As a p-type redox-active material, electrolyte anions are inserted concurrent with the oxidation of the **TAT-TA** COF as positive electrode material in a battery.

In order to investigate the performance of **TAT-TA** COF for charge storage in batteries, two types of electrodes were fabricated and investigated in Li half cells: conventional electrodes ("**TAT-TA** COF," henceforth) containing **TAT-TA** COF, acetylene black, and PVDF binder in a 30/50/20 wt % ratio coated on an Al current collector and free-standing electrodes prepared from **TAT-TA** COF and single-walled carbon nanotubes (SWCNTs) in a 1:2 weight ratio (named "**TAT-TA** COF/CNT") and used without current collector (Figures 3 and S13 for SEM images). The cyclic voltammograms [CVs, 1 M $LiPF_6$ in ethylene carbonate (EC)/dimethyl carbonate (DMC) 1:1 as electrolyte] show two reversible redox processes centered at half-wave potentials of 3.78 and 4.07 V vs Li/Li^+ for the **TAT-TA** COF/CNT electrodes (Figure 3a). The third oxidation of the azatruxene units (Figure 2a) could not be reversibly addressed in battery electrodes, likely because of irreversible side reactions in the higher potential range. The galvanostatic cycling data in Figure 3b,c clearly show a better performance for the **TAT-TA** COF/CNT compared with the conventional **TAT-TA** COF electrodes. Reversible specific discharge capacities of up to 70.4 mAh g^{-1} on the basis of the mass of the active material are accessible for the former at a 0.2 C rate, which corresponds to 82% of the theoretical specific capacity of 86.2 mAh g^{-1} assuming a two-electron transfer per azatruxene subunit. This is paired with an excellent rate performance (Figure 3b) where even at the fast rate of 20 C, 49 mAh g^{-1} are accessible. A long-term cycling at a rate of 2 C over 500 cycles confirms the excellent suitability of the azatruxene COF as a battery electrode material (Figure 3c). After stabilizing the cell at 0.2 C for 10 cycles, a specific discharge capacity of 68 mA h g^{-1} was obtained for the **TAT-TA** COF/CNT electrodes at a 2 C rate of which 76% was retained after 500 charge/discharge cycles. The SWCNTs only have a minor contribution to the capacity of 8 mAh g^{-1} (Figure S18). In comparison, the conventional **TAT-TA** COF electrodes show a retention of only 27% of the initial specific discharge capacity of 59 mAh g^{-1} obtained at 0.2 C in cycle 11 after 500 cycles at 2 C. Conventional electrodes with higher COF mass loadings of 40 and 50 wt % were also investigated and showed good performance but were inferior to the **TAT-TA** COF/CNT electrodes (Figure S19).

The charge/discharge profiles of the **TAT-TA** COF/CNT electrodes (Figure 3d) show a plateau area centered around 3.9 V vs Li/Li^+. This, as well as the clearly visible redox peaks in the CVs, prove a Faradaic charge storage behavior with anion insertion/deinsertion upon charge/discharge.[42]

The better performance of the **TAT-TA** COF/CNT electrodes can be rationalized by electrochemical impedance spectroscopy (EIS, Figure 3e). Compared with the conventional **TAT-TA** COF electrodes (220 Ω), the Nyquist plots of the **TAT-TA** COF/CNT electrodes show a significantly lower charge transfer resistance (80 Ω), indicated by the location of the semicircle, suggesting rapid charge transport capability due to an enhanced conductivity through the presence of the CNTs. To further investigate the electrochemical kinetics of the **TAT-TA** COF/CNT electrodes, CVs at different scan rates were measured, which showed that the redox processes are not limited by diffusion (Figure S15). The capacitive contribution amounts to 73% at a scan rate of 0.3 mV s^{-1} and increases to 87% at a scan rate of 2 mV s^{-1} (Figure S16), thereby further confirming the kinetically fast pseudocapacitive process during PF_6^- storage in **TAT-TA** COF/CNT. Galvanostatic intermittent titration technique (GITT) measurements confirmed that the porous structure of the COF improves ion transport through the electrode (Figure 3f). With values in the order of 10^{-8} cm^2 s^{-1}, the diffusion coefficients indicate fast and efficient anion diffusion, thereby showing that there is no diffusion limitation to the electrochemical redox reaction of the azatruxene COF.[43]

Next, the performance of the **TAT-TA** COF/CNT electrodes in Mg-based coin cells using metallic Mg as a counter electrode was investigated. As electrolyte, we used a 0.3 M solution of $Mg[B(hfip)_4]_2{\cdot}3DME$ in 1,2-dimethoxyethane (DME) as one of the best-working Mg electrolytes reported to date (Figure 4a).[23,26,44] The CV in the potential range of 2.0−3.5 V vs Mg/Mg^{2+} (Figure 4b) shows two redox events similar to the Li half cells. The half-wave potentials lie at 2.7 and 3.0 V, which is lower than in the Li system; however, these values closely correspond to the standard reduction potential difference between Mg and Li. This shows that the redox activity is also based in the azatruxene moieties. Moreover, the second redox process in the CV is characterized by a potential difference of ∼0.35 V between anodic and cathodic peak, which slightly decreases to ∼0.25 V with increasing cycle number, thereby implying relatively inferior electrochemical kinetics in the Mg cell in comparison with the Li half cells. Nevertheless, the overlap of the CV curves in the extended scans indicates highly reversible insertion of $[B(hfip)_4]^-$ anions in the positive electrode.

The Mg||**TAT-TA** COF/CNT cell shows excellent cycling behavior at fast C rates (Figure 4c). In the charge/discharge profiles at 5 C rate, the two redox events merge into one with a plateau centered at 2.9 V vs Mg/Mg^{2+}. This is in accordance with the differential specific capacity plots (Figure S20), which display broad peaks for both charge and discharge. These peaks indicate the (de)insertion of $[B(hfip)_4]^-$ anions into the **TAT-TA** COF/CNT electrode during (dis)charge. At a fast rate of 5 C corresponding to a current density of 655 mA g^{-1}, outstanding cycling stability is observed (Figure 4d). Of the initial 40 mAh g^{-1} specific discharge capacity corresponding to an energy density of 112 Wh kg^{-1} based on the active material, 84% is maintained over 1000 cycles. However, in comparison with the Li-based cells, the Mg cells exhibit a lower Coulombic efficiency of ∼87%. This might be partly attributed to the kinetic limitation of the Mg electrode redox reaction, which will be further investigated in separate studies. Nevertheless, the average discharge voltage of 2.9 V is higher than that of most reported Mg cells.[27,29] The cycling stability of the **TAT-TA** COF/CNT electrode in the Mg cell is higher than that in the Li cell, which might be related to the different electrolyte used. Dimethyl ether shows less reactivity toward the radical cations than carbonate solvents, which explains the higher stability.

CONCLUSIONS

With the synthesis and characterization of a crystalline and porous azatruxene COF, **TAT-TA** COF, employed as positive electrode material in Li half cells and Mg batteries, this work demonstrates that p-type COFs are competitive materials candidates for sustainable energy storage applications. The positive charges in the redox-active azatruxene units are stabilized by conjugation. The **TAT-TA** COF/CNT composite exhibits rapid charge transfer and high electrochemical accessibility of the redox active groups of **TAT-TA** COF. **TAT-TA** COF/CNT electrodes show high discharge potentials of 3.9 V vs Li/Li^+ and 2.9 V vs Mg/Mg^{2+} with a capacity retention of 76% (500 cycles at 2 C) and 84% (1000 cycles at 5 C), respectively, which makes this the first report of a p-type COF used in a Mg battery. It can be expected that installing anion-binding side chains as a structural modification will further amplify anion storage and ion mobility in such p-type COF materials. Furthermore, the design of highly conductive COFs and/or by performing in situ polycondensations on CNTs might reduce the required amount of conductive additives. The natural abundance and feasibility of the divalent Mg metal anode are particularly advantageous for cost-effective energy storage applications.

AUTHOR INFORMATION

Corresponding Authors

Birgit Esser − *Institute of Organic Chemistry II and Advanced Materials, Ulm University, D-89081 Ulm, Germany;* orcid.org/0000-0002-2430-1380; Email: birgit.esser@uni-ulm.de

Oliver Dumele − *Department of Chemistry & IRIS Adlershof, Humboldt-Universität zu Berlin, D-12489 Berlin, Germany; Institute of Organic Chemistry, University of Freiburg, 79104 Freiburg, Germany;* orcid.org/0000-0002-3277-6570; Email: oliver.dumele@oc.uni-freiburg.de

Authors

Sebastian M. Pallasch − *Department of Chemistry & IRIS Adlershof, Humboldt-Universität zu Berlin, D-12489 Berlin, Germany*

Manik Bhosale − *Institute of Organic Chemistry II and Advanced Materials, Ulm University, D-89081 Ulm, Germany*

Glen J. Smales − *Bundesanstalt für Materialforschung und -prüfung (BAM), 12205 Berlin, Germany;* orcid.org/0000-0002-8654-9867
Caroline Schmidt − *Institute of Organic Chemistry, University of Freiburg, 79104 Freiburg, Germany*
Sibylle Riedel − *Helmholtz Institute Ulm (HIU), 89081 Ulm, Germany*
Zhirong Zhao-Karger − *Helmholtz Institute Ulm (HIU), 89081 Ulm, Germany; Institute of Nanotechnology, Karlsruhe Institute of Technology, 76344 Eggenstein-Leopoldshafen, Germany;* orcid.org/0000-0002-7233-9818

Author Contributions

¶

S.M.P. and M.B. contributed equally.

Notes

The authors declare no competing financial interest.

ACKNOWLEDGMENTS

We thank Dr. Björn Kobin for measuring TGA, Dr. Lutz Grubert for assistance with solution-phase cyclic voltammetry and spectroelectrochemistry, Robin Wessling for support with electrochemical measurements, Sven Herter for measuring HRMS, and Prof. Philipp Adelhelm for access to SEM. O.D. is grateful to Stefan Hecht for his continuous support during the past years. This work was supported by the German Research Foundation through funding within the Priority Program SPP 2248 Polymer-Based Batteries (project number 441236036 and 441215516), the German Federal Ministry of Education and Research (BMBF BattFutur, 03XP0457), and the German Federal Environmental Foundation (DBU, graduate fellowship for C.S.). This work contributes to the research performed at CELEST (Center for Electrochemical Energy Storage Ulm-Karlsruhe) and was funded by the German Research Foundation (DFG) under Project ID 390874152 (POLiS Cluster of Excellence, EXC 2154).

REFERENCES

(1) Hager, M. D.; Esser, B.; Feng, X.; Schuhmann, W.; Theato, P.; Schubert, U. S. Polymer-Based Batteries—Flexible and Thin Energy Storage Systems. *Adv. Mater.* **2020**, *32*, 2000587.
(2) Massé, R. C.; Liu, C.; Li, Y.; Mai, L.; Cao, G. Energy storage through intercalation reactions: electrodes for rechargeable batteries. *Natl. Sci. Rev.* **2017**, *4*, 26−53.
(3) Zhu, D.; Xu, G.; Barnes, M.; Li, Y.; Tseng, C.-P.; Zhang, Z.; Zhang, J.-J.; Zhu, Y.; Khalil, S.; Rahman, M. M.; et al. Covalent Organic Frameworks for Batteries. *Adv. Funct. Mater.* **2021**, *31*, 2100505.
(4) Kim, J.; Kim, Y.; Yoo, J.; Kwon, G.; Ko, Y.; Kang, K. Organic batteries for a greener rechargeable world. *Nat. Rev. Mater.* **2023**, *8*, 54−70.
(5) Allendorf, M. D.; Dong, R.; Feng, X.; Kaskel, S.; Matoga, D.; Stavila, V. Electronic Devices Using Open Framework Materials. *Chem. Rev.* **2020**, *120*, 8581−8640.
(6) Esser, B. Redox Polymers as Electrode-Active Materials for Batteries. *Org. Mater.* **2019**, *01*, 063−070.
(7) Lu, Y.; Chen, J. Prospects of organic electrode materials for practical lithium batteries. *Nat. Rev. Chem.* **2020**, *4*, 127−142.
(8) Muench, S.; Wild, A.; Friebe, C.; Haupler, B.; Janoschka, T.; Schubert, U. S. Polymer-Based Organic Batteries. *Chem. Rev.* **2016**, *116*, 9438−9484.
(9) Gropp, C.; Canossa, S.; Wuttke, S.; Gándara, F.; Li, Q.; Gagliardi, L.; Yaghi, O. M. Standard Practices of Reticular Chemistry. *ACS Cent. Sci.* **2020**, *6*, 1255−1273.
(10) Schneemann, A.; Dong, R.; Schwotzer, F.; Zhong, H.; Senkovska, I.; Feng, X.; Kaskel, S. 2D framework materials for energy applications. *Chem. Sci.* **2021**, *12*, 1600−1619.
(11) Haldar, S.; Schneemann, A.; Kaskel, S. Covalent Organic Frameworks as Model Materials for Fundamental and Mechanistic Understanding of Organic Battery Design Principles. *J. Am. Chem. Soc.* **2023**, *145*, 13494−13513.
(12) Zhou, L.; Jo, S.; Park, M.; Fang, L.; Zhang, K.; Fan, Y.; Hao, Z.; Kang, Y.-M. Structural Engineering of Covalent Organic Frameworks for Rechargeable Batteries. *Adv. Energy Mater.* **2021**, *11*, 2003054.
(13) Cao, Y.; Wang, M.; Wang, H.; Han, C.; Pan, F.; Sun, J. Covalent Organic Framework for Rechargeable Batteries: Mechanisms and Properties of Ionic Conduction. *Adv. Energy Mater.* **2022**, *12*, 2200057.
(14) Yang, L.; Huang, N. Covalent organic frameworks for applications in lithium batteries. *J. Polym. Sci.* **2022**, *60*, 2225−2238.
(15) Hu, Y.; Wayment, L. J.; Haslam, C.; Yang, X.; Lee, S.-h.; Jin, Y.; Zhang, W. Covalent organic framework based lithium-ion battery: Fundamental, design and characterization. *EnergyChem.* **2021**, *3*, 100048.
(16) Luo, X.-X.; Wang, X.-T.; Ang, E. H.; Zhang, K.-Y.; Zhao, X.-X.; Lü, H.-Y.; Wu, X.-L. Advanced Covalent Organic Frameworks for Multi-Valent Metal Ion Batteries. *Chem.—Eur. J.* **2023**, *29*, No. e202202723.
(17) Esser, B.; Dolhem, F.; Becuwe, M.; Poizot, P.; Vlad, A.; Brandell, D. A perspective on organic electrode materials and technologies for next generation batteries. *J. Power Sources* **2021**, *482*, 228814.
(18) Lužanin, O.; Dantas, R.; Dominko, R.; Bitenc, J.; Souto, M. Tuning the electrochemical performance of covalent organic framework cathodes for Li- and Mg-based batteries: the influence of electrolyte and binder. *J. Mater. Chem. A* **2023**, *11*, 21553−21560.
(19) Wang, S.; Wang, Q.; Shao, P.; Han, Y.; Gao, X.; Ma, L.; Yuan, S.; Ma, X.; Zhou, J.; Feng, X.; et al. Exfoliation of Covalent Organic Frameworks into Few-Layer Redox-Active Nanosheets as Cathode Materials for Lithium-Ion Batteries. *J. Am. Chem. Soc.* **2017**, *139*, 4258−4261.
(20) Meng, Z.; Zhang, Y.; Dong, M.; Zhang, Y.; Cui, F.; Loh, T.-P.; Jin, Y.; Zhang, W.; Yang, H.; Du, Y. Readily useable bulk phenoxazine-based covalent organic framework cathode materials with superior kinetics and high redox potentials. *J. Mater. Chem. A* **2021**, *9*, 10661−10665.
(21) Wu, M.; Zhao, Y.; Zhao, R.; Zhu, J.; Liu, J.; Zhang, Y.; Li, C.; Ma, Y.; Zhang, H.; Chen, Y. Chemical Design for Both Molecular and Morphology Optimization toward High-Performance Lithium-Ion Batteries Cathode Material Based on Covalent Organic Framework. *Adv. Funct. Mater.* **2022**, *32*, 2107703.
(22) Liang, Y.; Dong, H.; Aurbach, D.; Yao, Y. Current status and future directions of multivalent metal-ion batteries. *Nat. Energy* **2020**, *5*, 646−656.
(23) Li, Z.; Häcker, J.; Fichtner, M.; Zhao-Karger, Z. Cathode Materials and Chemistries for Magnesium Batteries: Challenges and Opportunities. *Adv. Energy Mater.* **2023**, *13*, 2300682.
(24) Maroni, F.; Dongmo, S.; Gauckler, C.; Marinaro, M.; Wohlfahrt-Mehrens, M. Through the Maze of Multivalent-Ion Batteries: A Critical Review on the Status of the Research on Cathode Materials for Mg^{2+} and Ca^{2+} Ions Insertion. *Batter. Supercaps* **2021**, *4*, 1221−1251.
(25) Chen, Y.; Fan, K.; Gao, Y.; Wang, C. Challenges and Perspectives of Organic Multivalent Metal-Ion Batteries. *Adv. Mater.* **2022**, *34*, 2200662.
(26) Zhao-Karger, Z.; Liu, R.; Dai, W.; Li, Z.; Diemant, T.; Vinayan, B. P.; Bonatto Minella, C.; Yu, X.; Manthiram, A.; Behm, R. J.; et al. Toward Highly Reversible Magnesium−Sulfur Batteries with Efficient and Practical $Mg[B(hfip)_4]_2$ Electrolyte. *ACS Energy Lett.* **2018**, *3*, 2005−2013.

(27) Chen, Q.; Nuli, Y.-N.; Guo, W.; Yang, J.; Wang, J.-L.; Guo, Y.-G. PTMA/Graphene as a Novel Cathode Material for Rechargeable Magnesium Batteries. *Acta Phys. -Chim. Sin.* **2013**, *29*, 2295−2299.
(28) Ikhe, A. B.; Seo, J. Y.; Park, W. B.; Lee, J.-W.; Sohn, K.-S.; Pyo, M. 3-V class Mg-based dual-ion battery with astonishingly high energy/power densities in common electrolytes. *J. Power Sources* **2021**, *506*, 230261.
(29) Xiu, Y.; Mauri, A.; Dinda, S.; Pramudya, Y.; Ding, Z.; Diemant, T.; Sarkar, A.; Wang, L.; Li, Z.; Wenzel, W.; et al. Anion Storage Chemistry of Organic Cathodes for High-Energy and High-Power Density Divalent Metal Batteries. *Angew. Chem., Int. Ed.* **2023**, *62*, No. e202212339.
(30) DeBlase, C. R.; Silberstein, K. E.; Truong, T.-T.; Abruña, H. D.; Dichtel, W. R. *β*-Ketoenamine-Linked Covalent Organic Frameworks Capable of Pseudocapacitive Energy Storage. *J. Am. Chem. Soc.* **2013**, *135*, 16821−16824.
(31) Based on the accepted crystallinity criteria, see ref 9, an amorphous porous polymer in Mg-based batteries has been reported: Sun, R.; Hou, S.; Luo, C.; Ji, X.; Wang, L.; Mai, L.; Wang, C. A Covalent Organic Framework for Fast-Charge and Durable Rechargeable Mg Storage. *Nano Lett.* **2020**, *20*, 3880−3888.
(32) Pallasch, S.; Bhosale, M.; Smales, G. J.; Schmidt, C.; Riedel, S.; Zhao-Karger, Z.; Esser, B.; Dumele, O. A Porous Azatruxene Covalent Organic Framework as Positive Electrode Materials in Li- and Mg-based Batteries. *ChemRxiv*, August 3, 2023, ver. 2. DOI: 10.26434/chemrxiv-22023-k26492qw.
(33) Ji, L.; Fang, Q.; Yuan, M. S.; Liu, Z. Q.; Shen, Y. X.; Chen, H. F. Switching high two-photon efficiency: from 3,8,13-substituted triindole derivatives to their 2,7,12-isomers. *Org. Lett.* **2010**, *12*, 5192−5195.
(34) Goubard, F.; Dumur, F. Truxene: a promising scaffold for future materials. *RSC Adv.* **2015**, *5*, 3521−3551.
(35) Illicachi, L. A.; Urieta-Mora, J.; Calbo, J.; Aragó, J.; Igci, C.; García-Benito, I.; Momblona, C.; Insuasty, B.; Ortiz, A.; Roldán-Carmona, C.; et al. Azatruxene-Based, Dumbbell-Shaped, Donor−*π*-Bridge−Donor Hole-Transporting Materials for Perovskite Solar Cells. *Chem.—Eur. J.* **2020**, *26*, 11039−11047.
(36) Based on the accepted crystallinity criteria, see ref 9, an amorphous porous polymer has been reported: Xie, Y.-F.; Ding, S.-Y.; Liu, J.-M.; Wang, W.; Zheng, Q.-Y. Triazatruxene based covalent organic framework and its quick-response fluorescence-on nature towards electron rich arenes. *J. Mater. Chem. C* **2015**, *3*, 10066−10069.
(37) Yang, S.; Streater, D.; Fiankor, C.; Zhang, J.; Huang, J. Conjugation- and Aggregation-Directed Design of Covalent Organic Frameworks as White-Light-Emitting Diodes. *J. Am. Chem. Soc.* **2021**, *143*, 1061−1068.
(38) Li, X. C.; Zhang, Y.; Wang, C. Y.; Wan, Y.; Lai, W. Y.; Pang, H.; Huang, W. Redox-active triazatruxene-based conjugated microporous polymers for high-performance supercapacitors. *Chem. Sci.* **2017**, *8*, 2959−2965.
(39) Vitaku, E.; Dichtel, W. R. Synthesis of 2D Imine-Linked Covalent Organic Frameworks through Formal Transimination Reactions. *J. Am. Chem. Soc.* **2017**, *139*, 12911−12914.
(40) BIOVIA. *Material Studio*, 2022; Dassault Systèmes: San Diego, CA, 2022.
(41) Osterrieth, J. W. M.; Rampersad, J.; Madden, D.; Rampal, N.; Skoric, L.; Connolly, B.; Allendorf, M. D.; Stavila, V.; Snider, J. L.; Ameloot, R.; et al. How Reproducible are Surface Areas Calculated from the BET Equation? *Adv. Mater.* **2022**, *34*, 2201502.
(42) Gogotsi, Y.; Penner, R. M. Energy Storage in Nanomaterials − Capacitive, Pseudocapacitive, or Battery-like? *ACS Nano* **2018**, *12*, 2081−2083.
(43) Gannett, C. N.; Melecio-Zambrano, L.; Theibault, M. J.; Peterson, B. M.; Fors, B. P.; Abruña, H. D. Organic electrode materials for fast-rate, high-power battery applications. *Energy Rep.* **2021**, *1*, 100008.
(44) Ren, W.; Wu, D.; NuLi, Y.; Zhang, D.; Yang, Y.; Wang, Y.; Yang, J.; Wang, J. An Efficient Bulky $Mg[B(Otfe)_4]_2$ Electrolyte and Its Derivatively General Design Strategy for Rechargeable Magnesium Batteries. *ACS Energy Lett.* **2021**, *6*, 3212−3220.